Chromosome Translocations, Inversions and Telomere Length for Retrospective Biodosimetry on Exposed U.S. Atomic Veterans

Authors: McKenna, Miles J., Robinson, Erin, Taylor, Lynn, Tompkins, Christopher, Cornforth, Michael N., et al.

Chromosome Translocations, Inversions and Telomere Length for Retrospective Biodosimetry on Exposed U.S. Atomic Veterans

Miles J. McKenna,[a,b,c,1,2] Erin Robinson,[c] Lynn Taylor,[b] Christopher Tompkins,[c] Michael N. Cornforth,[a,d]
Steven L. Simon[e] and Susan M. Bailey[a,b,c]

[a] Cell and Molecular Biology Program and [b] Department of Environmental and Radiological Health Sciences, Colorado State University, Fort Collins, Colorado; [c] KromaTiD, Inc., Fort Collins, Colorado; [d] Department of Radiation Oncology, University of Texas Medical Branch, Galveston, Texas; and [e] Division of Cancer Epidemiology and Genetics, National Cancer Institute, National Institutes of Health, Bethesda, Maryland

McKenna, M. J., Robinson, E., Taylor, L., Tompkins, C., Cornforth, M. N., Simon, S. L. and Bailey, S. M. Chromosome Translocations, Inversions and Telomere Length for Retrospective Biodosimetry on Exposed U.S. Atomic Veterans. *Radiat Res*. 191, 311–322 (2019).

It has now been over 60 years since U.S. nuclear testing was conducted in the Pacific islands and Nevada, exposing military personnel to varying levels of ionizing radiation. Actual doses are not well-established, as film badges in the 1950s had many limitations. We sought a means of independently assessing dose for comparison with historical film badge records and dose reconstruction conducted in parallel. For the purpose of quantitative retrospective biodosimetry, peripheral blood samples from 12 exposed veterans and 12 age-matched (>80 years) veteran controls were collected and evaluated for radiation-induced chromosome damage utilizing directional genomic hybridization (dGH), a cytogenomics-based methodology that facilitates simultaneous detection of translocations and inversions. Standard calibration curves were constructed from six male volunteers in their mid-20s to reflect the age range of the veterans at time of exposure. Doses were estimated for each veteran using translocation and inversion rates independently; however, combining them by a weighted-average generally improved the accuracy of dose estimations. Various confounding factors were also evaluated for potential effects on chromosome aberration frequencies. Perhaps not surprisingly, smoking and age-associated increases in background frequencies of inversions were observed. Telomere length was also measured, and inverse relationships with both age and combined weighted dose estimates were observed. Interestingly, smokers in the non-exposed control veteran cohort displayed similar telomere lengths as those in the never-smoker exposed veteran group, suggesting that chronic smoking had as much effect on telomere length as a single exposure to radioactive fallout. Taken together, we find that our approach of combined chromosome aberration-based retrospective biodosimetry provided reliable dose estimation capability, particularly on a group average basis, for exposures above statistical detection limits. © 2019 by Radiation Research Society

INTRODUCTION

Biodosimetry entails assessment of biological markers of ionizing radiation exposure and is typically performed for the purpose of retrospectively reconstructing doses to individuals or populations. While there is a high level of interest in biodosimetry at short times after exposure (*2–4*), there are also important applications for biodosimetry at much longer times after exposure [see (*5, 6*)], particularly in the context of assessing doses and understanding their implications. Because the significance of a radiation exposure may not be fully appreciated at the time, and/or because other circumstances at the moment preclude collection of biological samples, many years may pass before such an assessment is undertaken. One of the few, true biodosimetric techniques with the capability for assessing dose many years after exposure is the quantitative evaluation of chromosome aberrations (*7, 8*). To derive an estimate of radiation dose received, aberration frequencies are used in conjunction with a calibration function (standard curve) that is specific to the population being studied. Prudent derivation of the calibration function (including a careful assessment of confounding factors that might affect aberration rates in the absence of radiation) are needed to derive realistic and reliable dose estimates.

Retrospective biodosimetry is of particular value in circumstances where physical dosimeters were not present at the time of exposure. This often applies to members of the public, where physical dose measurements are challenging, as well as to situations where theoretical (model-based) dose reconstruction is difficult. Furthermore, external dosimeters (even when present) can vary in accuracy (*9,*

10). Putting such obstacles aside, biodosimetry has intuitive appeal in that it assesses actual biological effects resulting from the radiation exposure. Biodosimetry-based dose reconstruction can be useful in helping to determine short-term care associated with acute radiation syndromes, as well as for assessing possible long-term medical sequelae (11) that may involve epidemiological studies, monetary compensation or redesign of radiation protection programs.

Here, we report approaches and findings utilizing chromosome aberration-based retrospective biodosimetry for estimation of radiation doses to U.S. military personnel who participated in nuclear testing activities after World War II. This analysis was conducted in support of the methodologic dose comparison study reported in a companion article (1), which compared and contrasted methods for assessing radiation dose decades after exposure.

Selection criteria for participants in the study included veterans of the U.S. armed forces or military contractors who had received the largest doses (>200 mSv) recorded by the Department of Defense and were still living (1). Participants had been exposed to radioactive fallout at either Rongerik Atoll, a site downwind of the Bikini Atoll test site in the Marshall Islands, or had participated in activities at the Nevada test site and/or the Pacific Proving Ground (other than Rongerik) in the 1950s leading to gamma (and occasionally, neutron) radiation exposure. These individuals provide a unique opportunity to evaluate the degree to which chromosome aberrations within a U.S. male adult population exposed more than six decades ago are sustained over time. Importantly, it also allows for comparisons to physical dose estimates based on film-badge dosimetry and/or model-based dose reconstruction (1).

The ''gold standard'' biodosimetric approach for relatively recent exposures (<1 year) involves evaluating frequencies of dicentric chromosomes in circulating blood lymphocytes (12, 13). Micronuclei also represent sensitive biomarkers of radiation exposure (14), and have been reported to persist more than five years after radioiodine therapy for papillary thyroid cancer (15). However, as is well known, both dicentrics and micronuclei result in large-scale loss of genetic information, and since such losses are often lethal to the cell, their frequencies decline over time (8, 16). Reciprocal translocations on the other hand can persist with time, so they have been used for exposures that occurred years to decades in the past (17). However, this approach is hampered by increases in translocation background frequencies associated with increasing age (18), as well as with lifestyle (e.g., smoking) and environmental (e.g., pesticides) factors, which complicate analyses (19). Moreover, it is unclear how long after exposure that chromosome aberrations can be evaluated and still result in reliable estimates of dose.

More recently, chromosomal inversions (inverted segments within the same chromosome) have been proposed as potential retrospective biodosimeters (20). Like reciprocal translocations (rearrangements between chromosomes), inversions represent symmetrical rearrangements (i.e., they are balanced), so they persist over time. However, due to the low-resolution of banding techniques historically used for their detection, the prevalence of inversions in disease and/or their value in biodosimetry is largely unknown. The strand-specificity of the emerging cytogenomics-based methodology of directional genomic hybridization (dGH) enables detection of inversions at much higher resolution than previously possible, while simultaneously also detecting translocations (21). Analyses of in vitro irradiated human cell lines and lymphocytes suggest that inversions are induced at a greater rate per unit dose than translocations, and further, that high-linear energy transfer (LET) particles are more efficient at inducing inversions than gamma rays (20, 22).

Telomeres, repetitive nucleoprotein caps that protect the physical ends of linear chromosomes, have also been proposed as biomarkers and/or predictors of radiation sensitivity (23, 24). Telomere length is influenced by a wide variety of cellular processes (e.g., cell division, oxidative stress), lifestyle factors (e.g., smoking, nutrition and exercise) and environmental exposures [e.g., ultraviolet (UV) and ionizing radiations], and so is an informative indicator of aging and overall health (25–27). We have previously proposed monitoring of telomere length dynamics (changes over time) together with inversion frequencies, as a means of evaluating radiation toxicity and normal tissue damage after radiation therapy (28).

In the context of the atomic veterans, we hypothesized that inclusion of inversions would improve the robustness of retrospective biodosimetry for estimating radiation doses that were received decades ago, as the persistence of inversions and their higher induction rate per unit dose would be favorable and exploitable qualities for dose estimation. Further, we speculated that telomere length might also reflect such previous exposures, thereby providing insight into long-term biological and overall health implications. Considering the constraint that we were limited to evaluations of chromosome aberrations many decades after exposure, we investigated five areas of interest: 1. whether persistent chromosome aberrations can give reliable dose estimates of radiation exposures that occurred in the past; 2. whether there is added value in combining chromosomal inversion and translocation frequencies for more reliable retrospective dose estimation; 3. whether frequencies of inversions, like translocations, are influenced by the covariates of age and smoking; 4. whether there is any relationship between telomere length and chromosome aberration based dose estimations; and 5. whether our approach can be employed to more reliably estimate individual or group doses received by living U.S. military veterans exposed approximately 60 years ago.

MATERIALS AND METHODS

Study Cohort

The study cohort consisted of two groups. One group (n = 12) was comprised of 10 U.S. military veterans and two civilian contractors to the military, all now 80–101 years of age, who, at the onset of this study (~2013), were believed to have each received 200 mSv or more from participation in nuclear testing-related activities, based on historical records of the Department of Defense. The other group served as a control group (n = 12) matched on similar military experience, gender and average age at time of enrollment. For simplicity, we will refer to these 24 military veterans, contractors and the control subjects, as ''veterans.'' In addition, six young adult males were recruited to provide blood samples for assay calibration purposes at approximately the same age (20–29 years of age) as the veteran cohort when they were exposed.

While 24 veterans were ultimately enrolled, 32 were originally selected. Of those, four were removed from the study due to illness or death and, therefore, their age-matched controls were also removed. Of the 24 veterans who ultimately participated, six were exposed to early radioactive fallout on Rongerik Atoll from the 1954 Castle Bravo detonation on Bikini Atoll, six others were believed to have been exposed at the Nevada test site (NTS) or other Pacific Proving Ground (PPG) locations, in various occupations, to prompt or delayed gamma radiation (*1*) and 12 were unexposed age-matched veteran control subjects. The subjects selected to participate in the control group were chosen, in part, to establish the same smoking frequency (58%) as among the exposed veterans (*1*). Typical of an aged cohort, a number of conditions and cancers were reported, but no one had received radiation therapy or chemotherapy (only surgery).

The young adult (control) group members selected by interview were generally healthy with no history of smoking, cancer or radiation exposure (e.g., radiotherapy or CT scans) and were of the same approximate age as the 12 exposed veterans at the time of their exposure in the 1950s. Three of the originally selected nine young adult males were excluded from the study due to the inability to stimulate their blood samples *ex vivo*. Thus, a total of six young adults were enrolled for purposes of generating calibration curves.

Sample Collection and Blood Stimulation

Peripheral blood from consenting volunteers was drawn and collected in 10-ml sodium heparin tubes (Becton, Dickinson and Co., Franklin Lakes, NJ) in accordance with NIH institutional review board approval [NIH Protocol 14CN170-C (SLS, PI)]. Samples were shipped under ambient conditions and received within 24 h of blood draw, then stimulated for 48–56 h at a 1:9 split in Gibco® PB-MAX™ Karyotyping Medium supplemented with phytohemagglutinin A (PHA; Thermo Fisher Scientific™ Inc., Rockford, IL). For directional genomic hybridization, 5.0 mM 5-bromo-deoxyuridine (BrdU) and 1.0 mM 5-bromo-deoxycytidine (BrdC) were added to the media, as described elsewhere (*21, 29*). At 4 h prior to harvest, KaryoMAX® Colcemid™ (Thermo Fisher Scientific) was added to a final concentration of 0.1 µg/ml. The stimulated blood was then harvested and metaphase chromosome spreads prepared using standard cytogenetic techniques (*30, 31*).

Irradiations for Calibration (Dose Response) Curves

Prior to stimulation, blood samples from the six young adult males were irradiated with acute doses of ^{137}Cs γ rays in a Mark I irradiator (JL Shepherd & Associates, San Fernando, CA) located at Colorado State University (Ft. Collins, CO). Chromosome aberration frequencies (determined by the methods described herein) were used to derive calibration curves at a series of dose points relevant to the expected exposure determinations: 0, 0.15, 0.25, 0.50, 1.0 and 2.0 Gy, delivered at a dose rate of 2.5 Gy/min. Sham-irradiated controls were kept under similar conditions (e.g., room temperature).

Directional Genomic Hybridization and Imaging

To simultaneously identify translocations and inversions, single-color whole chromosome 1, 2 and 3 dGH paints (KromaTiD Inc., Ft. Collins, CO) were used as previously described (*21, 29*). Briefly, slides containing metaphase spread preparations singly substituted with bromodeoxynucleotides (BrdU and BrdC) were submersed in Hoechst 33258 (Millipore Sigma, St. Louis, MO) for 15 min, selectively photolysed using a SpectroLinker™ UV Crosslinker (Spectroline®, Westbury, NY) equipped with 365-nm UV bulbs for 35 min, followed by exonucleolytic degradation of the nicked DNA with Exonuclease III (New England Biolabs® Inc., Ipswitch, MA) for 30 min. A hybridization mixture containing single-color (Cy-3 or Cy-3 equivalent, Atto-550) chromosome 1, 2 and 3 dGH paints (KromaTiD Inc.) was applied to the slides, which were cover-slipped and sealed with rubber cement, then denatured at 68°C for 3 min. Slides were hybridized overnight at 37°C followed by five washes in 2× SSC at 43°C prior to imaging. Metaphase spreads were imaged on a Nikon Eclipse Ni-U epifluorescence microscope equipped with an Andor's Zyla 5.5 sCMOS camera and SpectraX LED light source. Stacked images were taken of each metaphase spread composed of five images per stack with a step size of 0.3 µm. Over 200 metaphase spreads per veteran and 300 metaphase spreads per young adult were imaged and analyzed. Any clonal rearrangement that appeared two or more times was scored as one event.

DNA Isolation for Telomere Length Measurement

DNA was isolated from a minimum of 5×10^5 peripheral blood mononuclear cells (PBMCs) with the DNeasy Blood and Tissue Kit (QIAGEN®, Valencia, CA). PBMCs were initially incubated in proteinase K for 3 h at 37°C, rather than 10 min at 56°C as specified by the manufacturer. An average of 19.15 ± 3.41 ng/µl of DNA was isolated from each sample.

Multiplexed Quantitative PCR Telomere Length Measurement

Multiplexed quantitative PCR measurements of telomere length were performed as previously described (*32*). Briefly, a 22 µl of master mix was prepared using SYBR® Green GoTaq® qPCR Master Mix (Promega Inc., Madison, WI) combined with the telomere forward primer (TelG; 5′-ACACTAAGGTTTGGGTTT-GGGTTTGGGTTTGGGTTAGTGT-3′), telomere reverse primer (TelC; 5′-TGTTAGGTATCCCTATCCCTATCCCTATCCC-TATCCCT AACA-3′), albumin forward primer (AlbU; 5′-CGGCGGCGGGCGGCGCGGGCTGGGCGGA AATGCTGCA-CAGAATCCTTG-3′) and albumin reverse primer (AlbD; 5′-GCCCGGCCCGCCG CGCCCGTCCCGCCGGAAAAG-CATGGTCGCCTGTT-3′) at 10 µM per primer (Integrated DNA Technologies®, Coralville, IA) and RNase/DNase-free water. To the master mix, 3 µl of DNA at 3.33 ng/µl was added for a final volume of 25 µl. The TelG/C primers were at a final concentration of 900 nM and the AlbU/D primers at 400 nM.

Telomere length measurements were performed using a Bio-Rad® CFX-96 qPCR analysis machine (Hercules, CA). The cycle design was comprised of several steps: for step 1, one cycle at 95°C for 3 min to heat-activate the Taq polymerase; for step 2, two cycles at 94°C for 15 s and 49°C for 15 s to anneal and extend the telomere primers; and for step 3, 32 cycles at 94°C for 15 s, 62°C for 10 s, 74°C for 15 s, 84°C for 10 s and 88°C for 15 s to melt the early-amplified telomere products, followed by annealing and extension of the albumin primers. The melt curve was established by a 72–95°C ramp at 0.5°C/s increase with a 30-s hold. Multiplexing both telomere and albumin primers using a single fluorescent DNA-intercalating dye is possible, since the telomere primers amplify at a lower quantification cycle (Cq) than the albumin primers. Standard curves were prepared using human genomic DNA (Promega) with threefold dilutions ranging from 50 ng to 0.617 ng in 3 µl per dilution. Negative controls included a no-

TABLE 1
MDD (Gy) as a Function of Age Group, Smoking Status and Certainty Level

	25-year-old males		80–90-year-old males			
	Never-smokers		Never-smokers		Ever-smokers	
	95% (1.96 σ)	99% (2.575 σ)	95% (1.96 σ)	99% (2.575 σ)	95% (1.96 σ)	99% (2.575 σ)
Translocations	0.00	0.00	0.21	0.27	0.31	0.40
Inversions	0.50	0.66	0.16	0.21	0.18	0.24

Note. The MDD values apply specifically to the population groups studied.

template TelG/C only and AlbU/D only, and a combined TelG/C and AlbU/D control. Samples were normalized across plates using a human genomic DNA standard. Each sample was run in triplicate on a 96-well plate format and relative telomere length was established using a telomere (T) to albumin (A) ratio.

Numerical Analysis Methods

Extrapolation to whole-genome equivalency (WGE). Directional genomic hybridization whole chromosome paints were used to visualize translocations and inversions involving chromosomes 1, 2 and 3. Mathematical corrections were then employed to express total damage that was likely to have occurred throughout the genome (whole genome equivalency). For translocations, the correction for WGE considers exchanges between painted and unpainted (counterstained) chromosomes, as well as exchanges that occur among the uniquely painted chromosomes, whereas for inversions, the correction to WGE considers only intrachromosomal exchanges within the painted chromosomes themselves. Values for the genomic content of chromosomes, previously described elsewhere (*33, 34*), were used to determine the proportion of the genome painted (chromosomes 1, 2 and 3) as 0.223, which defined the correction factor applied to inversions. Using the approach outlined by Loucas *et al.* (*35*), a correction factor of 0.346 was employed for converting translocations to WGE. WGE correction is useful in that it gives "intuitive context" to the raw data provided by WCP (and dGH), and for that reason we have expressed the covariant data in that form. Nevertheless, it should be made clear that conversion of raw frequency data to WGE has no material effect on our ability to reconstruct the doses received by the atomic veterans; i.e., our results regarding dose reconstruction do not, in any way, rely on its use. Therefore, the raw aberration numbers (Supplementary Table S1; http://dx.doi.org/10.1667/RR15240.1.S1), rather than WGE, were used in the dose assessment and uncertainty analyses.

Estimating individual bone marrow dose and related uncertainty. Individual bone marrow dose is estimated due to fact that the aberrations observed in peripheral blood lymphoctyes were derived from exposed stem cells in the bone marrow. Radiation absorbed doses were estimated based on chromosome aberration rates (translocations or inversions) in each subject using the equation:

$$D_i = (AF_i - \overline{BF})/CF \quad (1)$$

Where,

D_i is absorbed dose (mGy) to bone marrow of individual *I*,
AF_i = measured aberration frequency (translocations or inversions) in peripheral blood lymphocytes from exposed subject *i*,
$\overline{BF}$ = average baseline aberration frequency derived independently for "ever-smoker" and "never-smoker" control subjects, and
CF = calibration factor equal to the slope of derived dose-response curve (aberration frequency/Gy).

Since each variable in the equation for dose estimation is associated with a potential error, an uncertainty analysis using the Monte Carlo method was employed to propagate the uncertainty by assigning a probability density function to each parameter. The observed counts of aberrations (AF) were assumed to follow a Poisson

distribution with a standard deviation equal to the mean, as was the mean baseline frequency $(\overline{BF})$. The probability density function of the calibration factor was determined directly from regression standard error of the slope. The Monte Carlo analysis was run for 50,000 iterations and produced a distribution of alternative values from which a mean and confidence interval could be derived directly from the simulation results.

Combined translocation and inversion dose. Because we derived a bone marrow dose using two independent[3] assays (translocations and inversions), we explored the possibility of estimating a single dose per subject based on data combined from both assays. The purpose of the combined assessment was to allow for the exploration of the strengths of the relationship between each individual assay, as well as the combined biodose, with other estimates of historical exposure, i.e., by historical film badges and model-based dose reconstruction (*1*). To estimate a single dose based on translocation and inversion frequencies simultaneously, we constructed the best linear unbiased estimate by the inverse variance weighting method (*36*). Basically, the dose estimates from translocations and inversions for each subject were inversely weighted by their respective measurement variance, thus incorporating information from each, but giving greater weight to the estimate having the greater precision, or conversely, the smaller uncertainty.

Estimation of the minimum detectable dose (MDD). Biodosimetry dose estimates can vary among individuals, even with the same exposure, because of the inherent biological variations among individuals, i.e., their predisposition to form aberrations after exposure, as well as statistical fluctuations associated with a finite number of cells sampled (scored). These sources of variation ultimately result in a MDD that can be detected for a specified confidence level and the number of cells scored.

In this study, the control and exposed groups consisted of individuals with similar life experiences, i.e., military service, gender, no occurrences of cancer or of having received therapeutic radiation treatments and of same approximate age. In addition, the exposed and control groups were matched by proportion of "ever" and "never" smokers. Thus, it could be reasonably assumed that control and exposed groups were subject to similar factors affecting the background frequencies of chromosome damage. The MDD in this particular study is the minimum acute dose of ionizing radiation necessary to induce a statistically significant increase in the number of aberrations or, equivalently, is the smallest dose at a specified confidence level that can be said to differ from a condition of *no added* exposure. We caution that the MDDs derived here are particular to the groups as defined in this study (80–90-year-old military veterans) and should not be generalized to other population groups.

Using the variability of aberration rates among the 12 nonexposed control subjects, we separately derived the MDD (see Table 1) for

---

[3] Occasionally, a complex exchange aberration can simultaneously involve a translocation and an inversion in such a way that they are obliged to have shared common breakpoints during their formation. In this case, the two end points may not be considered independent events. However, in our measurements, there was no statistically significant correlation between translocation and inversion frequencies within the exposed group or within the control group. For that reason, we considered the assays as statistically independent.
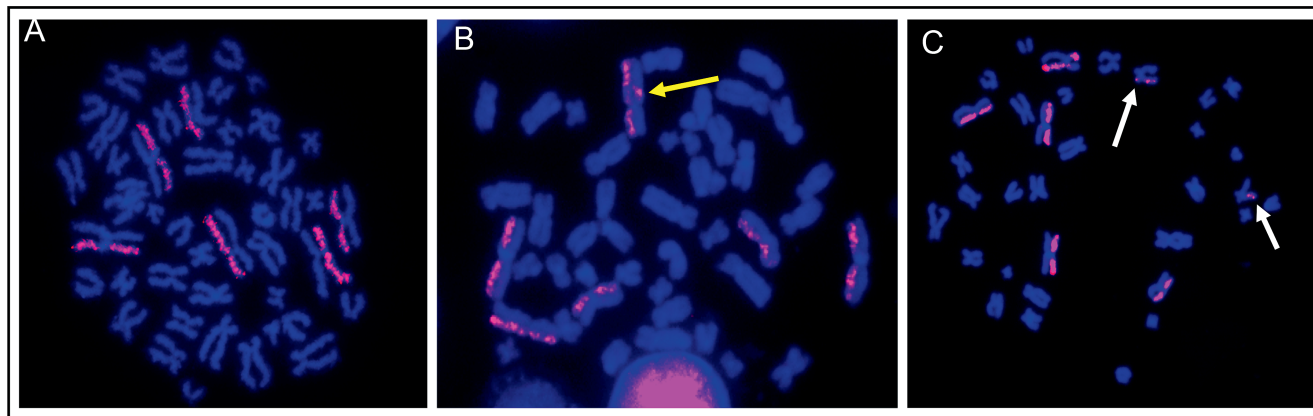
FIG. 1. Directional genomic hybridization (dGH). Representative images of metaphase spreads labeled with dGH whole chromosome 1, 2 and 3 paints (red) and counter stained with DAPI (blue). Panel A: A normal metaphase spread free of any structural rearrangements. dGH chromosome paints uniformly label a single sister chromatid of a chromosome. Panel B: An inversion (double signal switch; yellow arrow) on chromosome 2. Panel C: Translocation involving chromosome 3 and a second, unpainted chromosome (white arrows).

translocations and inversions using the procedure described by Tucker and Luckinbill (37), which generally follows the logic presented by the National Bureau of Standards (38) and later by Altshuler and Pasternak (39), as originally applied to estimates of minimum detectable radioactivity. Similar to estimating minimum detectable radioactivity, the main limiting factor is the variability of the background. Here it simply refers to the frequency of aberrations in the presumed absence of any added radiation exposure due to military service.

In simple terms, a multiple of the standard error, derived by the t distribution, is used to derive the minimum detectable radioactivity or MDD. Three sigma (σ = standard deviation of background) represents a confidence level of 99.7%. Less restrictive constraints, as shown in Table 1, are 95% confidence (1.96 σ) and 99% confidence (2.575 σ).

For the weighted translocation and inversion dose, an average of the MDD for the individual assays was used. Because the standard deviation of the translocation or inversion rate was found to vary according to smoking status, we derived a separate MDD according to smoking status.
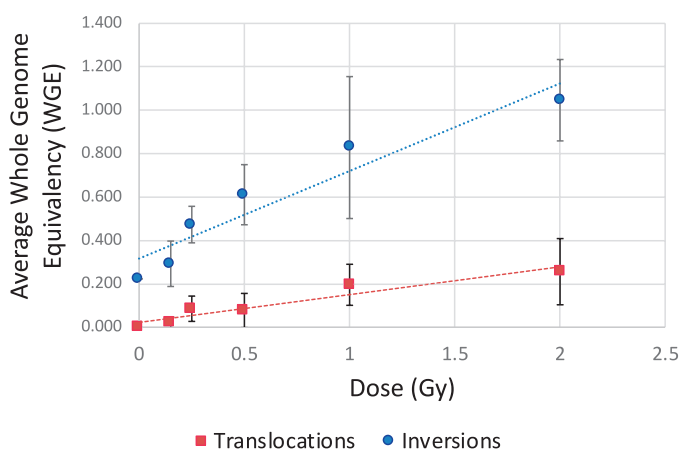
Minimum detectable doses are typically estimated for 95% or 99% confidence. MDD values are presented for both certainty levels in Table 1 with the 99% level used in all analyses. MDD values derived for translocations in this work (approximately 270 mGy for never-smokers at 99% certainty) were only slightly larger than published values [approximately 240 mGy (37)] involving larger data sets (18). To our knowledge, no estimates of the MDD for inversions have been previously reported.

RESULTS

Calibration (Dose Response) Curves

To establish radiation-induced dose-response relationships for translocations and inversions, whole peripheral blood samples from six young adults of approximately the same age as the study subjects at the time of exposure, were exposed *in vitro* to incrementally increasing acute doses of ^{137}Cs γ rays ranging from 0 Gy (controls) to 2.0 Gy. Translocations and inversions were quantified on metaphase spreads hybridized with whole chromosome 1, 2 and 3 dGH paints. On normal chromosomes devoid of structural rearrangements, dGH chromosome paints label a single sister chromatid (Fig. 1A); inversions are detected as a double signal "switch" between sister chromatids (Fig. 1B), and translocations identified by signal exchanges between chromosomes (Fig. 1C).

At the dose range interrogated for establishing calibration curves, both inversions and translocations individually displayed a dose response that was statistically consistent with linearity (Fig. 2). Consistent with previously reported *in vitro* findings (20), inversions were produced at a greater rate-per-unit dose than translocations, but also exhibited a higher spontaneous background rate. No translocations were identified in any of the young adult nonirradiated control samples analyzed (average age = 25 years, non-smokers), while inversions were detected at a background rate of 0.223 ± 0.124 aberrations per WGE.

FIG. 2. Calibration (dose-response) curves for young adult males; blood samples were exposed *in vitro* (^{137}Cs γ rays). The linear equations were y = 0.4037x + 0.3162 for inversions (blue) and y = 0.1281x + 0.022 for translocations (red). R-squared values were 0.9098 and 0.9091 for inversions and translocations, respectively. Error bars represent the standard deviation.

TABLE 2
Summary of Control Cohort Demographics and Covariate Influence on Background Translocation and Inversion Rates

	Young adults	Veteran control subjects (age-matched with exposed group)
Average age (years)	27 ± 2.3	85.75 ± 2.76
Smoker frequency	0/6	7/12
Non-smoker frequency	6/6	5/12
Ever-smokers		
Translocations per WGE	n/a	0.066 ± 0.053
Inversions per WGE	n/a	0.541 ± 0.192
Never-smokers		
Translocations per WGE	0	0.0636 ± 0.030
Inversions per WGE	0.223 ± 0.124	0.471 ± 0.104

Note. Aberration frequencies are corrected for whole genome equivalency (*35*).

Covariate Influence on Background Aberration Rates

Positive correlations of age and smoking with translocation frequencies are well established, with age being the greatest contributor to increases in background rates (*18, 19*). However, little is known regarding the influence of age and/or environmental and lifestyle factors on inversion frequencies. Here, baseline frequencies of translocations and inversions were established in the young adult and veteran control subjects according to covariate status (smoking and age) so that radiation doses among the exposed subjects could be derived with the greatest reliability. Table 2 summarizes the aberration frequencies observed in each subgroup.

Considering the influence of age alone between the young adult and veteran controls (Fig. 3), we observed a statistically significant increase in both inversion and translocation frequencies. Translocations increased by 0.065 ± 0.043 ($P = 0.0024$) between 25 and 85 years of age (average current age of exposed subjects). The increase cannot be quantified as a percentage increase since no translocations were detected in the 25-year-old group. Inversions increased by 0.289 ± 0.035 per WGE ($P = 0.0013$) between 25 and 85 years of age (average), i.e., approximately twofold among "ever" smokers, but could not be quantified as a percentage increase for "never" smokers. Baseline frequencies of both inversions and translocations (Fig. 4) in the 85-year-old control group was found to be larger among "ever" smokers compared to "never" smokers. A comparison of the aberration rates between "ever" smokers and "never" smokers suggested a 15% increase in baseline inversions, and a 3.8% increase in baseline translocation rates due to smoking. Comparisons were only made in the veteran control cohort since none in the young adult cohort reported smoking. Previously reported studies also support no statistically significant changes between smokers and non-smokers in their mid-20s (*18*).
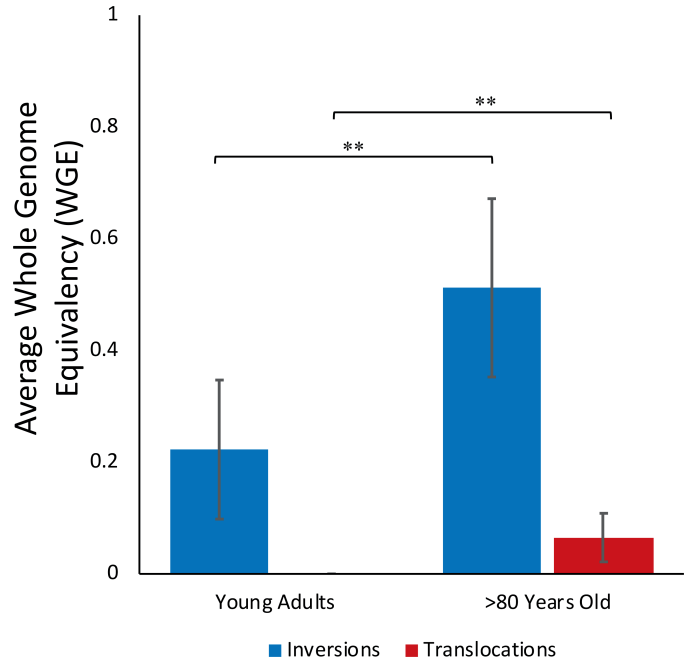

FIG. 3. Influence of age on background frequencies of inversions (blue) and translocations (red).

Observed Aberration Frequencies

Whole chromosome 1, 2 and 3 dGH paints were employed for simultaneous evaluation of both translocations and inversions. An average of 200 metaphase spreads per exposed veteran or age-matched control were scored (Supplementary Table S1; http://dx.doi.org/10.1667/RR15240.1.S1). Age-matched controls had an average of
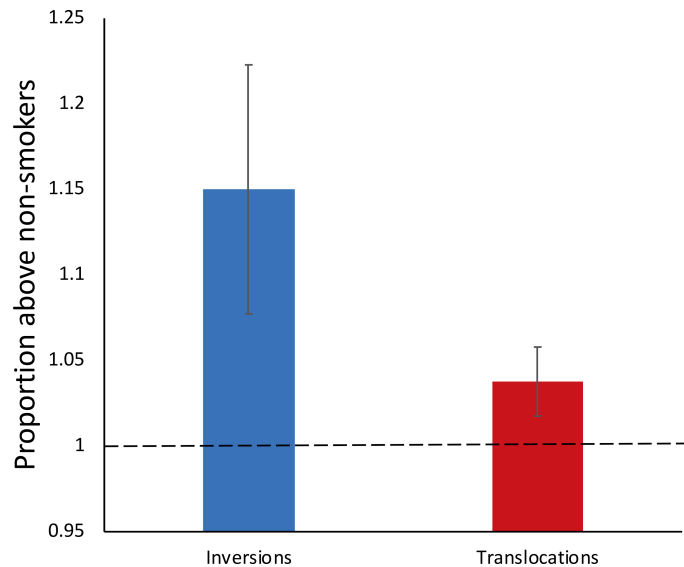

FIG. 4. Influence of smoking on background frequencies of inversions (blue) and translocations (red). The ratio of aberration rates between smokers and non-smokers in the veteran age-matched control cohort was used to obtain the proportional change in inversions and translocations. Error bars represent the standard error of the mean (SEM).

4.25 ± 2.98 translocations and 22.08 ± 8.08 inversions, while the exposed veterans had an average of 6.58 ± 4.62 and 26.08 ± 6.96 translocations and inversions, respectively. Notably, no translocations were seen in the 25-year-old group. However, an average background frequency of 2.5 ± 1.4 inversions was observed. While it is well established that age and smoking status influences translocation frequencies (*18*), this is the first report of age and smoking-related increases in background frequencies of inversions.

The observed aberration frequency is an important parameter, as it was directly used for dose and uncertainty estimations. Historically, this is one of the most common practices among published biodosimetric assessments (*12, 40, 41*).

Biodosimetry Assessment of Radiation Exposure to the Atomic Veterans

To estimate bone marrow doses based on inversion and translocation frequencies for each individual, the covariate influences on baseline frequencies were subtracted from the observed aberration frequencies, as in Eq. (1), $D_i = (R_i - \overline{BF})/CF$. Estimated radiation absorbed doses to active bone marrow (mGy) were established based on observed inversion or translocation frequencies independently (Fig. 5).

Estimates of a negative dose for either assay were below the MDD, although other dose estimates were found to be less than the MDD as well. Three out of six Rongerik veterans were below the MDD at the 95% confidence level, while four out of six were below the MDD at the 99% confidence level. Four out of six NTS/PPG veterans were below the MDD at both the 95% and 99% confidence level. We found that imputing one half the MDD for values <MMD, as suggested by the National Research Council (1989), significantly improved the comparison of group mean values of chromosome-based dose estimates with dose estimates based on film badges and dose reconstruction (*1*). This appears to be a useful strategy for replacement of values <MDD. Translocation and inversion rates (as assessed) were not correlated. Even so, many of the 95% confidence intervals (determined from uncertainty analysis) of inversion and translocation rates overlapped for individual veterans, suggesting that the dose estimates derived from the two aberration types were statistically comparable.

In an effort to possibly improve the reliability of dose estimates, we combined radiation-induced chromosome aberration frequencies for inversions and translocations (Fig. 5). As described earlier, we determined a weighted dose estimate as a best linear unbiased estimator where the inverse variance of each aberration rate was used as a weighting factor. Biodosimetry estimates of bone marrow dose for the Rongerik group and NTS/PPG groups, without correction for the <MDD, ranged from –47 to 740 mGy and –41 to 410 mGy, respectively. Negative
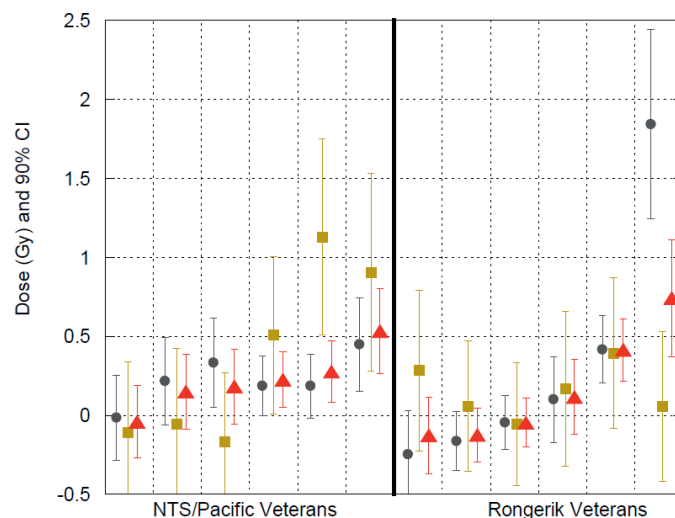

FIG. 5. Dose estimates and 90% confidence intervals for the Nevada Test Site, Pacific Proving Ground and Rongerik Atoll veterans. Each group of three estimations separated by a vertical dashed grid line represents a single individual. Dose estimates (Gy) for inversions (gold) and translocations (gray) were established independently. A combined estimate (red) was obtained by weighting inversion and translocation frequencies by their own inverse variance.

estimates could occur whenever the true dose was less than the MDD. After correction for <MDD (by imputation of one half the MDD for <MDD values), doses ranged from 120 to 740 mGy with a mean of 310 mGy for the Rongerik group, while the dose estimates for the NTS/PPG group ranged from 120 to 410 mGy with a mean of 225 mGy for the NTS/PPG group.

The weighted dose improved the chromosome aberration-based dose estimation (biodose) as judged by improved agreement between the biodose estimates and the model-based dose reconstruction; this approach was most successful after substituting one half the MDD value for weighted biodose estimates when they were less than that of the MDD. The correlation coefficient between the badge reading and dose reconstruction with translocation-based dose (r = 0.30) and inversion dose (r = 0.02) increased to r = 0.41 when the dose estimates were combined using the best linear unbiased estimator, and further increased to 0.58 when neutron exposures experienced by two of the 12 were accounted for in the dose reconstruction (*1*). These results suggest that for exposures that occurred decades in the past, a retrospective biodosimetry approach combining chromosomal inversion and translocation frequencies can provide a more reliable, and possibly more accurate, estimation of dose than translocations or inversions alone, although true doses must be above the MDD of the assay. Furthermore, the correlations suggest that agreement between biodosimetry and other methods is most successful at the group average level rather than at the individual level. Agreement of dose estimates from different methods for the same individual is greatly limited by measurement imprecision and, in many cases, missing data.
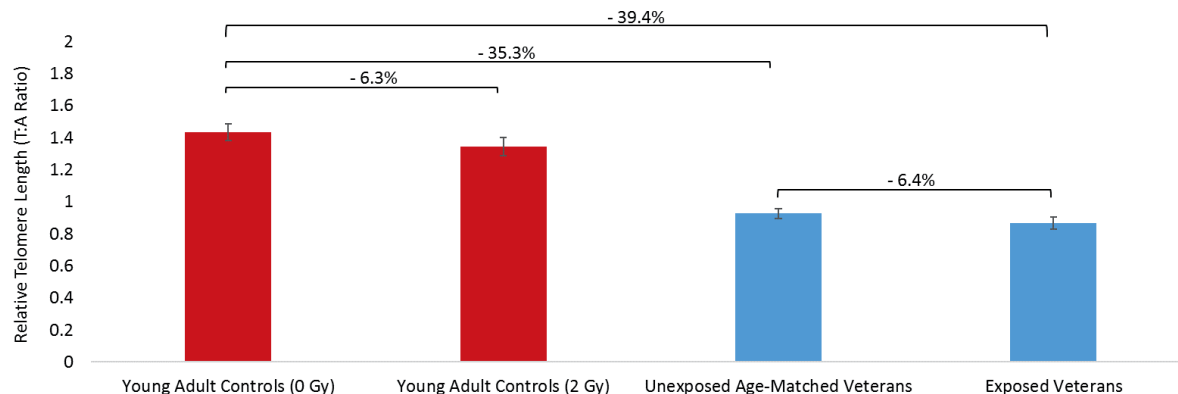
FIG. 6. Relative telomere length in cohorts based on age and radiation exposure; young adults (red) and veterans (blue). Values between bars represent percentage change between groups. Error bars represent SEM.

Estimation of Minimum Detectable Dose

Multiple assessments of inversion and translocation background frequencies were made utilizing samples from the six mid-20-year-old male control subjects. The standard error of the mean aberration rate was determined as an estimate of the standard deviation of the ''mean sampling distribution.'' This analysis suggested that the MDD for the exposed veterans varies for the experimental design described above, from approximately 0.21 to 0.40 Gy for translocations, depending on the certainty level and smoking status. It varied from approximately 0.16 to 0.24 Gy for inversions, depending on certainty level and smoking status (Table 1).

Influence of Age, Smoking and Radiation Exposure on Telomere Length

Telomere length represents an informative and particularly relevant biomarker of aging, general health, lifestyle factors and stresses, as well as environmental exposures (*42*). However, very little is known in regard to the long-term effects on telomere length in human populations after exposure to ionizing radiation, as highlighted by conflicting results in the few studies that have been reported (*26, 43*).

Here, a multiplexed quantitative PCR (qPCR) based approach (*32*) was employed to establish relative telomere length for each sample. As expected, comparison of telomere length between the young adult controls (mid-20 years of age) and the veteran controls (>80 years of age) demonstrated that age was the largest contributing factor to telomere shortening, irrespective of smoking status or radiation exposure (Fig. 6). A 35.3% and 39.4% decrease in telomere length was observed between the unexposed (0 Gy) young adult controls and the unexposed ($P < 0.0001$) and exposed veterans ($P < 0.0001$), respectively. Although not statistically significant, a 6.3% decrease in telomere length occurred between the 0 and 2.0 Gy *in vitro* γ-ray irradiated young adult control samples. Similarly, a 6.4% decrease was observed between the unexposed and *in vivo* exposed veterans.

Assessment of the influence of smoking status on telomere length in the unexposed compared to the exposed veterans also proved interesting. Age-matched veteran controls who reported a history of chronic smoking appeared to have decreased telomere length (T:A ratio = 0.874 ± 0.163) that was similar to both the exposed non-smoker (T:A ratio 0.871 ± 0.285) and exposed-smoker (T:A ratio = 0.865 ± 0.165) veteran cohorts (Fig. 7). These results suggest that chronic smoking over several decades results in telomere attrition similar to that of individuals exposed to a low-dose nuclear event. There did not appear to be any additive effect of a history of chronic smoking and radiation exposure.

Lastly, there was a weak negative correlation ($r = -0.399$) between telomere length and the weighted combined translocation and inversion dose estimations (Fig. 8), lending support to the notion that low-dose ionizing radiation exposures have long-lasting effects on overall health. Atomic veterans with a negative dose estimation were considered to be below the limits of detection, and so were removed from the analysis.

DISCUSSION

The most intuitive method to confirm biodose estimates would be to directly compare individual estimates against measurements from physical dosimeters. In the case of U.S. veterans exposed in the 1950s and 1960s, personnel monitoring badges were often not issued on an individual basis, and only approximately 25% of men were issued badges (*44*). Many men were assigned readings based on a single badge for a member of their military unit in which all members tended to perform similar duties. In addition to the problem of a lack of physical measurements on an individual basis, badges do not necessarily reflect bone marrow dose since, not only is the badge located superficially on the body, there may be differences in shielding of individuals during the time of exposure. For these reasons, there is little opportunity for direct comparisons of our biodose estimates with physical dosimetry

FIG. 7. Relative telomere length and smoking status and/or radiation exposure in the veteran cohorts. Error bars represent SEM.

measurements. Herein, we compare our biodose estimates with dose estimates from Simon *et al*. (*1*) that were based on film badge readings when available and supplemented by dose reconstruction calculations. As discussed, comparisons of our biodose estimates also depend on recognition of those estimates <MDD and replacement of those values with the most unbiased values. Even considering such constraints, several significant findings emerged from the use of our chromosome-based approaches for retrospective biodosimetry on exposed U.S. atomic veterans.

Chromosomal signatures of radiation exposure remain for more than 60 years. We find that U.S. military veterans exposed to radioactive fallout and gamma radiation from activities associated with atomic bomb testing still exhibit a

biological signature that includes chromosomal translocations, as well as inversions, and to a lesser extent, telomere shortening. Our findings are consistent with a published study of Japanese fishermen exposed to the same nuclear test near Bikini Atoll (CASTLE Bravo) in 1954 as the Rongerik veterans, in which stable chromosome aberrations (evaluated by G-banding) remained elevated above background levels (*45*). Moreover, Simon *et al*. (*1*) has shown that after correction for those estimates <MDD, the chromosome aberration-based estimates correlated well with dose estimates determined by other strategies. These various findings support that radiation exposure signatures in the form of chromosome aberrations are still detectable approximately 60 years after exposure and, with proper interpretation strategies, can provide reliable or, at least, consistent estimates of radiation dose.

Chromosome inversion and translocation combinations improve dose estimation. Although translocations have been evaluated extensively for the purpose of retrospective biodosimetry, e.g., in atomic bomb survivors (*46*), Chernobyl clean-up workers (*47*) and for occupational exposures (*8*), to our knowledge, this is the first reported study utilizing inversions as informative biomarkers of prior radiation exposure in a human population. Consistent with our previously published *in vitro* studies (*20*), we found that inversions were induced at a greater rate-per-unit dose (0.404/WGE/Gy) than translocations (0.133/WGE/Gy). Of relevance to radiation-related cancer risk, we note that inversions and their alternative outcome, interstitial deletions, are the two most common mutational signatures associated with radiation-induced secondary malignancies (*48*). It is worth noting that background frequencies of inversions were significantly higher than those of translo-
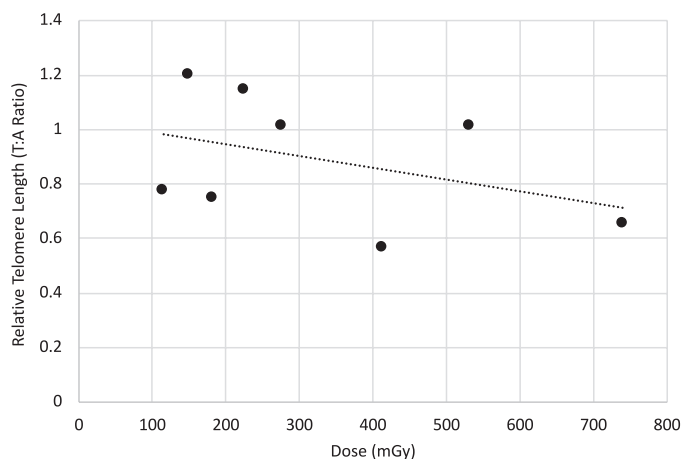

FIG. 8. Relative telomere length as a function of weighted combined chromosome aberration dose among exposed veterans. The linear equation is y = –0.0004x + 1.0324 and $R^2 = 0.1599$.

cations (0.223 ± 0.124/CE vs. 0), possibly reflective of the proposed role spontaneous inversions play in reorganizing the genome (*49*).

Covariates of age and smoking influence inversion frequencies. Interestingly, age and smoking status influenced both translocation as well as inversion background frequencies. Compared to the young-adult controls, the veteran controls showed a 0.289 ± 0.035/WGE increase in inversions and a 0.065 ± 0.043/WGE increase in translocations. That is, inversions increased 2.3-fold in the >80-year-old individuals compared to the young adults. Likewise, smoking status was directly correlated with background aberration frequencies, as a 15% (0.0706/WGE) increase in inversions and a 3.77% (0.0024/WGE) increase in translocations was attributable to smoking alone.

While advancing age and smoking are known to increase translocation frequencies, to our knowledge this is the first reported study of age and smoking status influencing background inversion frequencies. While these confounding factors would be expected to negatively affect the utility of inversions for retrospective biodosimetry, the greater induction rate of inversions per unit dose appeared to be advantageous in that, when combined with translocation rates, more reliable dose estimates were obtained.

Inverse relationship between telomere length and weighted combined dose estimates. Telomere length was measured for all exposed and control participants in the study. It is well established that telomere length erosion occurs with cellular division and, therefore, with aging, limiting the replicative lifespan of somatic cells. This reduced replicative capacity has been proposed as a tumor suppressor mechanism, since it prevents aberrant cell survival (*50*). Not only have short telomeres been associated with a host of age-related diseases, such as cardiovascular disease (*51*) and cancer (*52*), they are also indicative of radiosensitivity (*23, 24*), suggesting value for the use of telomere length dynamics as an informative biomarker of general health, as well as environmental exposures.

Consistent with reports from atomic bomb survivors (*43*), an inverse relationship between telomere length and exposure to ionizing radiation was observed, further supporting the use of telomeres as valuable biomarkers to be included in the context of radiation exposure. Telomere length averaged across all exposed samples suggested an ∼ 6% decrease compared to unexposed controls. Moreover, when telomere length for each individual was evaluated compared to their weighted average utilizing both translocations and inversions to estimate dose, the inverse relationship with escalating dose was readily apparent. Interestingly, long-term, chronic smoking shortened telomeres as much as a single exposure to ionizing radiation from atomic bomb testing. We also believe this to be the first report of telomere shortening associated with human

exposure to radioactive fallout, as evidenced by the exposures of the Rongerik group.

Inversions improve individual radiation dose estimates. To estimate radiation doses for exposed study participants, doses were based on independently-assessed translocation and inversion frequencies using an inverse-variance weighted method that combined both data sets. Effects of both age and smoking were adjusted prior to estimating dose and propagating uncertainty. Depending on the certainty level chosen for the MDD, 50% to 67% of the estimates were <MDD, making interpretations of point estimates and confidence intervals difficult. Regardless, nine of 12 analyzed samples had overlapping mean values and/or variances, suggesting that both aberrations were statistically comparable. In contrast, three individuals did not have overlapping variances, suggestive of differences in individual susceptibilities. To improve sensitivity and minimize variance, both translocations and inversion dose estimates were combined by a best linear unbiased estimator based on inverse variance weighting. In general, compared to inversions, translocations had a lower variance relative to the mean across all samples, thus, more weight was placed on the translocation rate than on the inversion rates.

As per our published companion piece (*1*), the inverse variance-weighted estimates were better correlated with estimates from dose reconstruction and had the smallest systematic differences on a group level than either translocations or inversions alone. While this finding tends to suggest that combined translocation and inversion rates provide more reliable and potentially more accurate dose estimations for retrospective biodosimetry than either end point alone, this analysis needs to be evaluated in other studies before a firm conclusion can be drawn. There is a possibility that this finding may be unique to this situation where exposures occurred many years in the past.

Finally, we have estimated the average absorbed doses for the Rongerik and NTS/PPG veterans to be approximately 310 mGy and 225 mGy, respectively, both in good agreement with dose reconstruction (inclusive of a neutron RBE when necessary) and reported as equivalent doses (mSv) in (*1*). Details of the comparisons between chromosome-based dose estimates and various retrospective dose estimation strategies (for the same study participants) can be found in Simon *et al.* (*1*).

We conclude that chromosome aberration-based retrospective biodosimetry gave acceptable dose estimation capability, on average, for exposures above the statistical detection limits, even if received more than six decades earlier. Moreover, we conclude that these techniques may be useful in other radiation scenarios, e.g., those that might occur today or in the future involving accidental or intentional exposures. This research responds to the challenge set forth by Simon and Bouville (*53*) for the development and improvement of methods that can be used at long times after radiation exposure. Additional experi-

ence in applying these and similar techniques will undoubtedly improve our capability to more reliably estimate past exposures.

SUPPLEMENTARY INFORMATION

Table S1. Observed translocations and inversions per 200 cells for whole chromosome 1, 2 and 3 dGH paints and estimated bone marrow doses (mGy).

ACKNOWLEDGMENTS

REFERENCES

1. Simon SL, Bailey SM, Beck HL, Boice JD, Bouville A, Brill AB, et al. Estimation of radiation doses to U.S. military veterans from nuclear testing: A comparison of historical film-badge measurements, dose reconstruction, and retrospective biodosimetry. Radiat Res 2019; 297–310:191.

2. Alexander GA, Swartz HM, Amundson SA, Blakely WF, Buddemeier B, Gallez B, et al. BiodosEPR-2006 Meeting: Acute dosimetry consensus committee recommendations on biodosimetry applications in events involving uses of radiation by terrorists and radiation accidents. Radiat Meas 2007; 42:972–96.

3. Rezaeejam H, Shirazi A, Valizadeh M, Izadi P. Candidate gene biodosimeters of mice and human exposure to ionizing radiation by quantitative reverse transcription polymerase chain reaction. J Cancer Res Ther 2015; 11:549–57.

4. Zeegers D, Venkatesan S, Koh SW, Low GKM, Srivastava P, Sundaram N, et al. Biomarkers of Ionizing Radiation Exposure: A Multiparametric Approach. Genome Integr 2017; 8:6. (https://bit.ly/2FjFojs)

5. Ionizing radiation exposure of the population of the United States. NCRP Report No. 160. Bethesda, MD: National Council on Radiation Protection and Measurements; 2009. (https://bit.ly/2FibfRp)

6. Simon SL, Bailiff I, Bouville A, Fattibene P, Kleinerman RA, Lloyd DC, et al. BiodosEPR-2006 consensus committee report on biodosimetric methods to evaluate radiation doses at long times after exposure. Radiat Meas 2007; 42:948–71.

7. Camparoto ML, Ramalho AT, Natarajan AT, Curado MP, Sakamoto-Hojo ET. Translocation analysis by the FISH-painting method for retrospective dose reconstruction in individuals exposed to ionizing radiation 10 years after exposure. Mutat Res 2003; 530:1–7.

8. Cho MS, Lee JK, Bae KS, Han E-A, Jang SJ, Ha W-H, et al. Retrospective biodosimetry using translocation frequency in a stable cell of occupationally exposed to ionizing radiation. J Radiat Res (Tokyo) 2015; 56:709–16.

9. Simon SL, Bouville A, Kleinerman R. Current use and future needs of biodosimetry in studies of long-term health risk following radiation exposure. Health Phys 2010; 98:109–17.

10. Suntharalingam N, Cameron JR. A Comparison of TLD and film for personnel dosimetry. Health Phys 1966; 12. (https://bit.ly/2FhdEfi)

11. Rea ME, Gougelet RM, Nicolalde RJ, Geiling JA, Swartz HM. Proposed triage categories for large-scale radiation incidents using high-accuracy biodosimetry methods. Health Phys 2010; 98:136–44.

12. Rothkamm K, Beinke C, Romm H, Badie C, Balagurunathan Y, Barnard S, et al. Comparison of established and emerging biodosimetry assays. Radiat Res 2013; 180:111–9.

13. Vaurijoux A, Gruel G, Roch-Lefevre S, Voisin P. Biological dosimetry of ionizing radiation. In: Nenoi M, editor. Current topics in ionizing radiation research. Rijeka, Croatia: INTECH Open Access Publisher; 2012. (https://bit.ly/2SGZcjL)

14. Lloyd DC. Chromosomal analysis to assess radiation dose. Stem Cells 1997; 15:S195–201.

15. Livingston GK, Khvostunov IK, Gregoire E, Barquinero J-F, Shi L, Tashiro S. Cytogenetic effects of radioiodine therapy: a 20-year follow-up study. Radiat Environ Biophys 2016; 55:203–13.

16. Tucker JD, Cofield J, Matsumoto K, Ramsey MJ, Freeman DC. Persistence of chromosome aberrations following acute radiation: I, PAINT translocations, dicentrics, rings, fragments, and insertions. Environ Mol Mutagen 2005; 45:229–48.

17. Tawn EJ, Whitehouse CA. Persistence of translocation frequencies in blood lymphocytes following radiotherapy: implications for retrospective radiation biodosimetry. J Radiol Prot Off J Soc Radiol Prot 2003; 23:423–30.

18. Sigurdson AJ, Ha M, Hauptmann M, Bhatti P, Sram RJ, Beskid O, et al. International study of factors affecting human chromosome translocations. Mutat Res Toxicol Environ Mutagen 2008; 652:112–21.

19. Ramsey MJ, Moore DH, Briner JF, Lee DA, Olsen LA, Senft JR, et al. The effects of age and lifestyle factors on the accumulation of cytogenetic damage as measured by chromosome painting. Mutat Res 1995; 338:95–106.

20. Ray FA, Robinson E, McKenna M, Hada M, George K, Cucinotta F, et al. Directional genomic hybridization: inversions as a potential biodosimeter for retrospective radiation exposure. Radiat Environ Biophys 2014; 53:255–63.

21. Ray FA, Zimmerman E, Robinson B, Cornforth M, Bedford J, Goodwin E, et al. Directional genomic hybridization for chromosomal inversion discovery and detection. Chromosome Res 2013; 21:165–74.

22. Cornforth MN, Durante M. Radiation quality and intra-chromosomal aberrations: Size matters. Mutat Res Toxicol Environ Mutagen 2018; 836(Pt A):28–35.

23. Goytisolo FA, Samper E, Martín-Caballero J, Finnon P, Herrera E, Flores JM, et al. Short telomeres result in organismal hypersensitivity to ionizing radiation in mammals. J Exp Med. 2000; 192:1625–36.

24. Wong KK, Chang S, Weiler SR, Ganesan S, Chaudhuri J, Zhu C, et al. Telomere dysfunction impairs DNA repair and enhances sensitivity to ionizing radiation. Nat Genet 2000; 26:85–8.

25. Cherkas LF, Hunkin JL, Kato BS, Richards JB, Gardner JP, Surdulescu GL, et al. The association between physical activity in leisure time and leukocyte telomere length. Arch Intern Med. 2008; 168:154–8.

26. Reste J, Zvigule G, Zvagule T, Kurjane N, Eglite M, Gabruseva N, et al. Telomere length in Chernobyl accident recovery workers in

the late period after the disaster. J Radiat Res (Tokyo) 2014; 55:1089–100.

27. Valdes AM, Andrew T, Gardner JP, Kimura M, Oelsner E, Cherkas LF, et al. Obesity, cigarette smoking, and telomere length in women. Lancet Lond Engl 2005; 366:662–4.

28. McKenna MJ, Bailey SM. Chromosomal and telomeric biomarkers of normal tissue injury to evaluate risk of degenerative health effects (secondary malignancy, cardiovascular disease) post radiation therapy. Transl Cancer Res 2017; 6:S789–94.

29. Robinson E, McKenna MJ, Bedford JS, Goodwin EH, Cornforth MN, Bailey SM, et al. Directional Genomic Hybridization (dGH®) for Detection of Intra-Chromosomal Rearrangements. Radiat Cytogen: Meth Mol Biol 2019. (in press)

30. Howe B, Umrigar A, Tsien F. Chromosome preparation from cultured cells. J Vis Exp 2014:e50203.

31. Williams ES, Cornforth MN, Goodwin EH, Bailey SM. CO-FISH, COD-FISH, ReD-FISH, SKY-FISH. In: Songyang Z, editor. Telomeres and telomerase: methods and protocols. Totowa, NJ: Humana Press; 2011. p. 113–24.

32. Cawthon RM. Telomere length measurement by a novel monochrome multiplex quantitative PCR method. Nucleic Acids Res 2009; 37:e21–e21.

33. Mayall BH, Carrano AV, Moore DH, Ashworth LK, Bennett DE, Mendelsohn ML. The DNA-based human karyotype. Cytometry 1984; 5:376–85.

34. Morton NE. Parameters of the human genome. Proc Natl Acad Sci U S A. 1991 Sep 1;88:7474–6.

35. Loucas BD, Shuryak I, Cornforth MN. Three-color chromosome painting as seen through the eyes of mFISH: another look at radiation-induced exchanges and their conversion to whole-genome equivalency. Front Oncol 2016; 6:52. (https://bit.ly/2QC5j73)

36. Hartung J, Knapp G, Sinha BK. Statistical meta-analysis with applications. Hoboken, NJ: Wiley; 2008.

37. Tucker JD, Luckinbill LS. Estimating the lowest detectable dose of ionizing radiation by FISH whole-chromosome painting. Radiat Res 2011; 175:631–7.

38. A manual of radioactivity procedures - NBS Handbook 80. Gaithersburg, MD: National Bureau of Standards; 1961. p. 27.

39. Altshuler B, Pasternack B. Statistical measures of the lower limit of detection of a radioactivity counter. Health Phys 1963; 9:293–8.

40. Badie C, Kabacik S, Balagurunathan Y, Bernard N, Brengues M, Faggioni G, et al. NATO biodosimetry study. Radiat Res 2013; 180:138–48.

41. Straume T, Lucas JN, Tucker JD, Bigbee WL, Langlois RG. Biodosimetry for a radiation worker using multiple assays. Health Phys 1992; 62:122–30.

42. Shammas MA. Telomeres, lifestyle, cancer, and aging. Curr Opin Clin Nutr Metab Care 2011; 14:28–34.

43. Lustig A, Shterev I, Geyer S, Shi A, Hu Y, Morishita Y, et al. Long term effects of radiation exposure on telomere lengths of leukocytes and its associated biomarkers among atomic-bomb survivors. Oncotarget 2016; 7:38988–98.

44. Till JE, Beck HL, Aanenson JW, Grogan HA, Mohler HJ, Mohler SS, et al. Military participants at U.S. atmospheric nuclear weapons testing— methodology for estimating dose and uncertainty. Radiat Res 2014; 181:471–84.

45. Tanaka K, Ohtaki M, Hoshi M. Chromosome aberrations in Japanese fishermen exposed to fallout radiation 420–1200 km distant from the nuclear explosion test site at Bikini Atoll: report 60 years after the incident. Radiat Environ Biophys 2016; 55:329–37.

46. Kodama Y, Pawel D, Nakamura N, Preston D, Honda T, Itoh M, et al. Stable chromosome aberrations in atomic bomb survivors: results from 25 years of investigation. Radiat Res 2001; 156:337–46.

47. Snigiryova G, Braselmann H, Salassidis K, Shevchenko V, Bauchinger M. Retrospective biodosimetry of Chernobyl clean-up workers using chromosome painting and conventional chromosome analysis. Int J Radiat Biol 1997; 71:119–27.

48. Behjati S, Gundem G, Wedge DC, Roberts ND, Tarpey PS, Cooke SL, et al. Mutational signatures of ionizing radiation in second malignancies. Nat Commun 2016; 7:12605.

49. Kirkpatrick M. How and why chromosome inversions evolve. PLoS Biol 2010; 8:e1000501.

50. Deng Y, Chan SS, Chang S. Telomere dysfunction and tumour suppression: the senescence connection. Nat Rev Cancer 2008; 8:450–8.

51. Serrano AL, Andres V. Telomeres and Cardiovascular Disease. Circ Res 2004; 94:575–84.

52. Artandi SE, DePinho RA. Telomeres and telomerase in cancer. Carcinogenesis 2010; 31:9–18.

53. Simon SL, Bouville A. Long-term biodosimetry redux. Radiat Prot Dosimetry 2016; 172:244–7.